Trends in the Torsional Potentials of Methoxy and Trifluoromethoxy Groups: An ab Initio and Density Functional Study on the Structure of para-Substituted Pyridines and Pyridinium Cations

Johanna Klocker, Alfred Karpfen,* and Peter Wolschann

Institute for Theoretical Chemistry and Structural Biology, University of Vienna, Währinger Strasse 17, A-1090 Vienna, Austria

Received: December 4, 2002; In Final Form: February 4, 2003

The structures and the torsional potentials around the aryl-O bond of 4-methoxypyridine, 4-trifluoromethoxypyridine, 4-methoxypyridinium cation, and 4-trifluoromethoxypyridinium cation were studied systematically with the aid of large-scale ab initio calculations performed at the Møller−Plesset second-order level and with a density functional method. In all compounds, the most stable conformer corresponds to the structure in which the methoxy or the trifluoromethoxy group is in an eclipsed conformation, oxygen and carbon atoms coplanar with the pyridine ring. The highest barrier to rotation, about 9.0 kcal mol^{-1}, is predicted for 4-methoxypyridinium cation at an orthogonal conformation with a torsional angle of 90°. The lowest torsional barrier, less than 1 kcal mol^{-1}, is obtained for 4-trifluoromethoxypyridine. The systematic variations of the calculated torsional potentials of these compounds are compared to those recently computed for methoxy- and trifluoromethoxybenzene and for their para-deprotonated anions. The trends in the energy differences between eclipsed and orthogonal conformations are correlated with concomitant changes of some of the optimized geometrical parameters in this series. Particularly suited are the two carbon−oxygen distances forming the ether linkage, and even more so their difference. The simple and astonishingly regular structural and energetic trends in this series can be rationalized by the assumption of a systematic decrease of the conjugation of the arene with the methoxy and trifluoromethoxy groups upon going from the 4-methoxypyridinium cation to the para-deprotonated trifluoroanisole anion.

1. Introduction

Not much is known about the structures and the torsional potentials of the various conceivable 4-methoxy- and 4-trifluoromethoxyheteroarenes. Solely the two parent compounds, methoxybenzene (MB) or anisole, and trifluoromethoxybenzene (TFMB) or α,α,α-trifluoroanisole have been intensively investigated, the latter only quite recently. Experimental investigations of the vibrational spectra of MB, in particular the torsional frequency of the methoxy group,[1,2] and gas-phase structure determinations with the aid of electron diffraction[3] and microwave spectroscopy,[4] have shown that the methoxy group in MB has a conformation with the carbon atom and the oxygen atom located in the plane of the benzene ring. From both electron diffraction and microwave data, it was concluded that only one stable conformer exists. The more recent theoretical calculations on the structure and torsional potential of MB[5−10] confirm the picture of a minimum for the *eclipsed* conformation (torsional angle $\phi = 0°$, [e]-form) and a very flat maximum at the *orthogonal* conformation ($\phi = 90°$, [o]-form). See Figure 1 for a sketch of the [e]- and [o]-forms of MB. In the most accurate calculations available so far,[7,9,10] a barrier height close to 3 kcal mol^{-1} has been reported.

In sharp contrast to the case of MB, TFMB has an equilibrium structure in which the $-OCF_3$ group is oriented orthogonally to the benzene ring. This has been shown by recent gas electron diffraction, microwave, and vibrational spectroscopic investigations[11,12] and by a number of theoretical studies.[8,10−12] Apart from the global [o]-form minimum, there is, however, a second, low-lying minimum corresponding to the [e]-form with a comparatively small energy difference of about 0.25−0.45 kcal mol^{-1} and a low energy barrier between these two conformers. This picture emerges from density functional theory calculations[8,10−12] and from Møller−Plesset second-order (MP2) calculations with extended basis sets.[10] From the two experimental studies[11,12] no clear consensus about the existence of this second minimum and the shape of the torsional potential could be achieved.

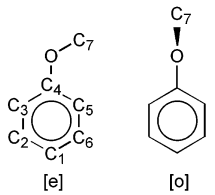

Figure 1. [e]- and [o]-conformations of MB and atomic numbering scheme.

In the previous work of this series,[10] the structures and the torsional potentials of the hypothetical anions of MB and TFMB, as obtained by deprotonation at the para-position, have also been investigated in some detail. The aim of these investigations was to accurately describe and to elucidate the modifications of the torsional potential upon going from MB to TFMB, and to correlate these changes with some characteristic alterations of bond distances or bond angles. The two most sensitive structural parameters turned out to be the aryl-O and the $O-CR_3$ (R═

* To whom correspondence should be addressed. Tel: (+43-1) 4277-52760. FAX: (+43-1) 4277-9527. E-mail: Alfred.Karpfen@univie.ac.at.

10.1021/jp0276146 CCC: $25.00
Published on Web 03/06/2003

TABLE 1: Selected Optimized Geometry Parameters of MP and TFMP at [e]- and [o]-Conformations as Obtained at MP2/cc-pVTZ and B3LYP/cc-pVTZ Levels[a]

	MP				TFMP			
	[e]-form		[o]-form		[e]-form		[o]-form	
	B3LYP	MP2	B3LYP	MP2	B3LYP	MP2	B3LYP	MP2
C4−C3[b]	1.396	1.396	1.390	1.391	1.387	1.388	1.383	1.386
C2−C3	1.382	1.386	1.389	1.392	1.386	1.389	1.390	1.392
C2−N	1.339	1.344	1.334	1.340	1.334	1.340	1.333	1.339
N−C6	1.330	1.336	1.334	1.340	1.331	1.337	1.333	1.339
C5−C6	1.392	1.395	1.389	1.392	1.392	1.394	1.390	1.392
C4−C5	1.393	1.394	1.390	1.391	1.387	1.389	1.383	1.386
C4−O	1.353	1.354	1.372	1.372	1.387	1.384	1.400	1.396
O−C7	1.423	1.421	1.428	1.426	1.356	1.356	1.356	1.356
C2−C3−C4	118.6	118.8	118.3	118.4	117.9	118.2	117.4	117.4
N−C2−C3	124.2	124.3	123.9	124.0	123.9	124.0	123.8	124.0
C2−N−C6	116.4	115.9	117.0	116.6	116.9	116.3	117.4	116.9
N−C6−C5	124.6	124.8	123.9	124.0	124.5	124.8	123.8	124.0
C4−C5−C6	118.1	118.2	118.3	118.4	117.2	117.2	117.4	117.4
C3−C4−C5	118.1	118.0	118.7	118.7	119.6	119.4	120.3	120.2
C3−C4−O	116.7	116.7	120.6	120.6	114.9	114.8	119.6	119.7
C5−C4−O	125.2	125.2	120.7	120.7	125.5	125.8	120.0	120.0
C4−O−C7	118.6	116.2	115.1	112.0	122.0	119.7	118.2	115.4
C5−C4−O−C7	0.0	0.0	90.0	90.0	0.0	0.0	90.0	90.0

[a] Bond distances in Å and angles in degrees. [b] For numbering, see Figure 1 (N replaces C1).

TABLE 2: Selected Optimized Geometry Parameters of MP^+ and $TFMP^+$ Cations at [e]- and [o]-Conformations as Obtained at MP2/cc-pVTZ and B3LYP/cc-pVTZ Levels[a]

	MP^+				$TFMP^+$			
	[e]-form		[o]-form		[e]-form		[o]-form	
	B3LYP	MP2	B3LYP	MP2	B3LYP	MP2	B3LYP	MP2
C4−C3[b]	1.412	1.408	1.404	1.401	1.403	1.400	1.396	1.394
C2−C3	1.363	1.370	1.371	1.379	1.367	1.374	1.374	1.381
C2−N	1.355	1.352	1.350	1.347	1.351	1.348	1.348	1.347
N−C6	1.348	1.345	1.350	1.347	1.347	1.345	1.348	1.347
C5−C6	1.369	1.377	1.371	1.379	1.372	1.379	1.374	1.381
C4−C5	1.410	1.407	1.404	1.401	1.402	1.400	1.396	1.394
C4−O	1.312	1.316	1.332	1.339	1.341	1.343	1.360	1.363
O−C7	1.446	1.443	1.454	1.449	1.403	1.397	1.394	1.389
C2−C3−C4	119.6	119.8	119.4	119.5	119.2	119.5	118.6	118.7
N−C2−C3	120.1	119.8	119.8	119.4	119.8	119.5	119.7	119.3
C2−N−C6	121.9	122.3	122.6	123.1	122.2	122.7	123.0	123.5
N−C6−C5	120.6	120.3	119.8	119.4	120.5	120.3	119.7	119.3
C4−C5−C6	119.0	119.1	119.4	119.5	118.4	118.5	118.6	118.7
C3−C4−C5	118.7	118.7	119.1	119.2	119.7	119.6	120.5	120.6
C3−C4−O	116.3	116.2	120.2	120.3	114.7	114.5	119.5	119.5
C5−C4−O	125.1	125.1	120.5	120.5	125.6	125.9	119.8	119.8
C4−O−C7	120.9	118.4	119.0	114.7	122.5	120.1	119.2	115.8
C5−C4−O−C7	0.0	0.0	90.0	90.0	0.0	0.0	90.0	90.0

[a] Bond distances in Å and angles in degrees. [b] For numbering, see Figure 1 (N replaces C1).

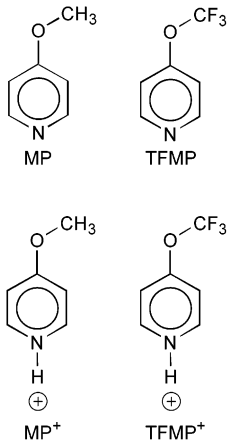

Figure 2. Schematic structures of the molecules treated in this work.

H,F) distances of these four molecules. It could be shown that both C−O bond length changes correlate very directly with the energy difference between [e]- and [o]-conformations. Whereas

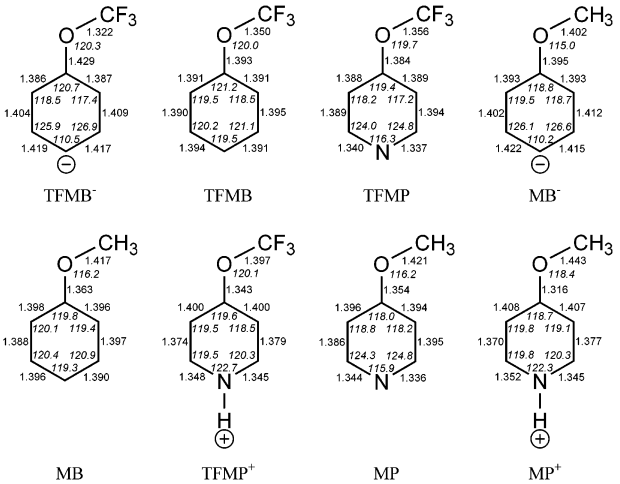

Figure 3. MP2/cc-pVTZ-optimized structural parameters of MB, MB^-, TFMB, $TFMB^-$, MP, MP^+, TFMP, and $TFMP^+$ (bond distances in angstroms, angles in degrees). The structures of MB, MB^-, MP, and MP^+ are taken from ref 10.

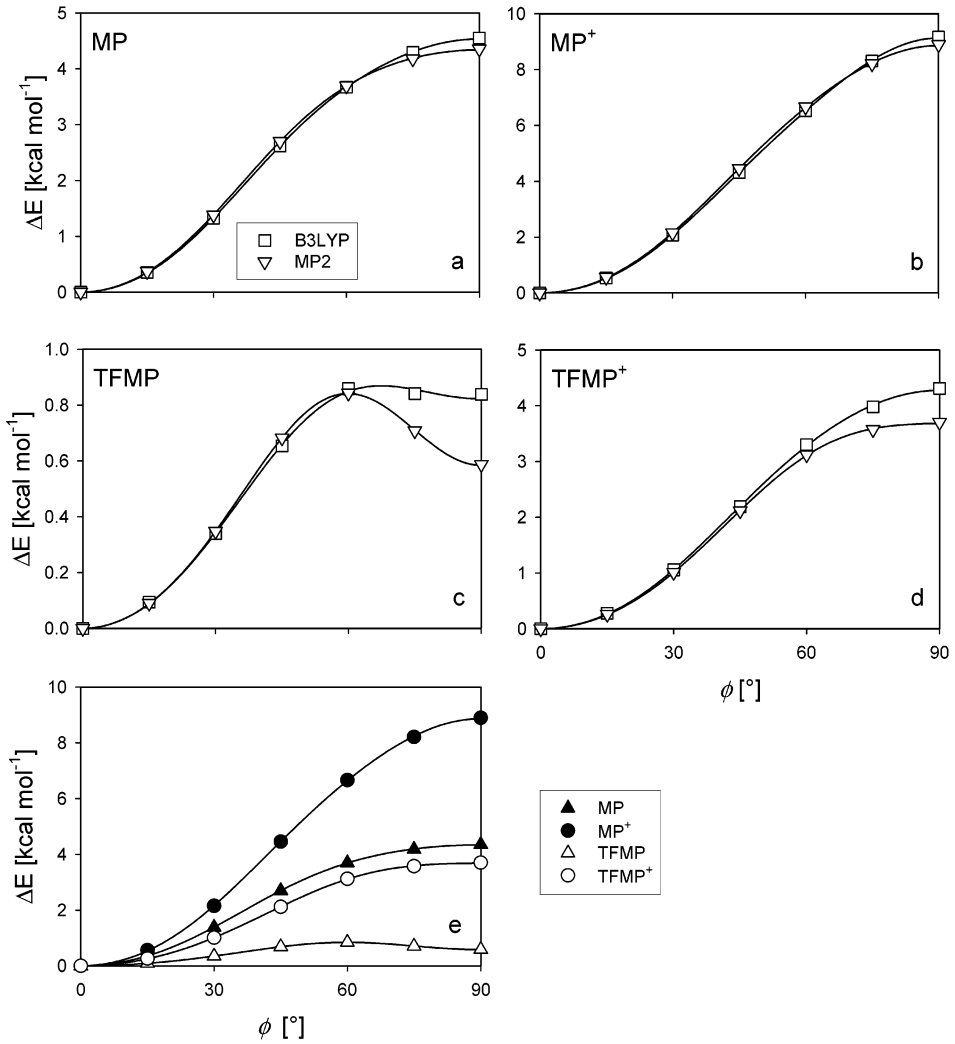

Figure 4. MP2/cc-pVTZ- and B3LYP/cc-pVTZ-calculated torsional potentials of (a) MP, (b) MP^+, (c) TFMP, (d) $TFMP^+$, and (e) a comparison of all four MP2/cc-pVTZ potential curves.

the mere existence of this correlation is perhaps not too surprising, the regularity of this interdependence is indeed astonishing, in particular the fact that it persists, even when the energetic preferences for either the [e]- or the [o]-conformation are reversed.

In this work, we continue the systematic investigations of the torsional potentials of methoxy and trifluoromethoxy groups adjacent to aromatic rings. We present the results of high-level ab initio and density functional calculations on the structures and on the torsional potentials of 4-methoxypyridine (MP), 4-trifluoromethoxypyridine (TFMP), and the corresponding pyridinium cations MP^+ and $TFMP^+$ (see Figure 2). To the best knowledge of the authors, there are no published experimental data pertinent to the structures and torsional potentials of these molecules available nor was this issue addressed in previous theoretical calculations. The data obtained in this work are compared to those reported previously for MB, MB^-, TFMB, and $TFMB^-$.[10]

The aim of this work is to provide a coherent picture of the trends in the torsional potentials of methoxy and trifluoromethoxy groups attached to benzene and to the para-positions of phenyl anion, pyridine, and pyridinium cation over a wide range of barrier heights and to correlate these barrier heights with systematic changes in the most important geometry parameters, in particular, the two C−O single bonds forming the ether linkage.

2. Method of Calculation

All quantum chemical calculations were performed with the Gaussian 98 suite of programs.[13] As basis sets, the correlation-consistent (aug)-cc-pVnZ[14−18] basis sets of Dunning and coworkers were selected. The ab initio calculations were performed at the Møller−Plesset second-order (MP2) level.[19] Density functional theory calculations were done with the hybrid B3LYP[20−23] variant as implemented in *Gaussian 98*.

For all four molecules, complete structure optimizations were carried out at the MP2 and B3LYP levels applying cc-pVDZ, aug-cc-pVDZ, and cc-pVTZ basis sets. Full optimization of all geometry parameters, with the exception of the fixed torsional angle, was also applied for the calculation of the torsional potentials. A regular grid of 15°−30° was used in the region from 0° to 90°. Where affordable, single-point MP2/aug-cc-pVTZ, MP2/cc-pVQZ, B3LYP/aug-cc-pVTZ, and B3LYP/cc-pVQZ calculations were also carried out at the respective cc-pVTZ-optimized geometries.

The pointwise-calculated torsional potential energies were subjected to simple Fourier fits

$$V(\phi) = \sum_{i=1}^{m} \frac{1}{2} V_n (1 - \cos n\phi); \quad n \text{ even.}$$

Fits extended up to the V_8 term turned out to be sufficient in all

TABLE 3: MP2- and B3LYP-Calculated Relative Energies of MP, MP^+, TFMP, and $TFMP^+$ at $\phi = 0$, 30, 60, and 90° as Obtained with Basis Sets of Increasing Size (kcal mol^{-1})

		B3LYP, ϕ				MP2, ϕ			
	basis set	0°	30°	60°	90°	0°	30°	60°	90°
MP	cc-pVDZ	0	1.34	3.73	4.52	0	1.30	3.41	3.90
	aug-cc-pVDZ	0	1.33	3.77	4.63	0	1.22	3.30	3.74
	cc-pVTZ	0	1.32	3.67	4.55	0	1.38	3.70	4.35
	aug-cc-pVTZ	0	1.28	3.58	4.52	0	1.34	3.53	4.14
	cc-pVQZ	0			4.55	0			4.35
MP^+	cc-pVDZ	0	2.09	6.64	9.26	0	2.09	6.49	8.61
	aug-cc-pVDZ	0	2.09	6.66	9.26	0	2.02	6.30	8.28
	cc-pVTZ	0	2.07	6.54	9.17	0	2.15	6.66	8.90
	aug-cc-pVTZ	0	2.06	6.49	9.11	0	2.09	6.50	8.69
	cc-pVQZ	0			9.17	0			8.89
TFMP	cc-pVDZ	0	0.24	0.68	0.68	0	0.22	0.46	0.06
	aug-cc-pVDZ	0	0.37	0.90	0.89	0	0.25	0.49	0.08
	cc-pVTZ	0	0.34	0.86	0.84	0	0.35	0.84	0.59
	aug-cc-pVTZ	0	0.33	0.83	0.83	0	0.29	0.73	0.43
	cc-pVQZ	0			0.86	0			0.59
$TFMP^+$	cc-pVDZ	0	0.96	3.10	4.20	0	0.90	2.75	3.21
	aug-cc-pVDZ	0	1.08	3.33	4.33	0	0.92	2.74	3.11
	cc-pVTZ	0	1.06	3.30	4.31	0	1.01	3.12	3.70
	aug-cc-pVTZ	0	1.05	3.26	4.29	0	0.96	3.02	3.55
	cc-pVQZ	0			4.33	0			3.70
MB	cc-pVTZ[a]	0	1.05	2.73	3.15	0	1.12	2.79	3.03
MB^-	cc-pVTZ[a]	0	0.42	0.69	0.37	0	0.64	1.05	0.69
TFMB	cc-pVTZ[a]	0.28	0.39	0.37	0	0.44	0.55	0.56	0
$TFMB^-$	cc-pVTZ[a]	1.74	1.49	0.73	0	1.66	1.47	0.79	0

[a] Reference 10.

TABLE 4: MP2/cc-pVTZ- and B3LYP/cc-pVTZ-Calculated Fourier Fit Parameters of MP, MP^+, $TFMP^+$, and TFMP (kcal mol^{-1})

		V2	V4	V6	V8
MP^+	B3LYP	9.04	−0.25	0.09	−0.10
MP		4.58	0.35	−0.04	−0.04
$TFMP^+$		4.33	0.06	−0.05	−0.02
TFMP		0.89	0.25	−0.06	0.00
MP^+	MP2	8.90	0.03	−0.03	−0.07
MP		4.43	0.53	−0.09	−0.04
$TFMP^+$		3.85	0.28	−0.17	0.01
TFMP		0.72	0.39	−0.13	0.01

cases considered, the difference between calculated and fitted energies not exceeding 12 cm^{-1}. At the [e]- and [o]-conformations, harmonic vibrational frequencies were calculated at the B3LYP/cc-pVTZ level in order to verify the nature of minima and saddle points.

3. Results and Discussion

The most important geometry parameters of the MP2/cc-pVTZ- and B3LYP/cc-pVTZ-optimized structures of MP and TFMP [o]- and [e]-forms are compiled in Table 1, those of MP^+ and $TFMP^+$ in Table 2. In general, the agreement between MP2- and B3LYP-optimized structures is quite good. The only exception is the C4−O−C7 bond angle, for which the B3LYP-optimized value is a few degrees larger than the MP2 counterpart. The very same systematic deviation has been observed for MB, TFMB, MB^-, and $TFMB^-$, too.[10] Details of the MP2/cc-pVTZ-optimized structural parameters, including those of MB, TFMB, MB^-, and $TFMB^-$ are given in Figure 3. In the course of the rotation of methoxy or trifluoromethoxy groups around the aryl-O bond, the three bond angles C3−C4−O, C5−C4−O, and C4−O−C7 change significantly, and the C4−O distance is slightly lengthened upon going from the [e]- to the [o]-form, whereas the remaining geometry parameters are hardly modified.

Substantial differences are encountered when the C4−O and O−C7 bond lengths are compared for the four molecules. The MP2-calculated C4−O/O−C7 bond length pairs at the [e]-conformation are 1.354/1.421 Å for MP, 1.384/1.356 for TFMP, 1.316/1.443 for MP^+, and 1.343/1.397 for $TFMP^+$, respectively. The corresponding B3LYP numbers follow closely the same trend. Thus, in the series MP^+, $TFMP^+$, MP, and TFMP, the C4−O distance is systematically stretched. The reverse trend is observed for O−C7 in the series MP^+, MP, $TFMP^+$, and TFMP. Overall, a very wide range of C−O single-bond distances is covered in this series. A useful geometry parameter for the following discussion is also the bond length difference Δr(C−O) defined as C4−O−O−C7. At the MP2/cc-pVTZ level, this parameter adopts the values −0.127, −0.067, −0.054, and 0.028, respectively, when choosing the order MP^+, MP, $TFMP^+$, and TFMP in the above series. Again the corresponding B3LYP/cc-pVTZ-calculated Δr(C−O) adopts very similar values: −0.134, −0.070, −0.062, and 0.031.

The MP2/cc-pVTZ- and B3LYP/cc-pVTZ-calculated torsional potentials of the four molecules are displayed in Figure 4. The highest barrier is obtained for MP^+ (see Figure 4b) with values close to 9 kcal mol^{-1}. The lowest barrier, less than 1 kcal mol^{-1}, is calculated for TFMP (see Figure 4c). In the case of TFMP, the [o]-conformation is a flat minimum at the MP2/cc-pVTZ level. The barrier of about 0.8 kcal mol^{-1} relative to the [e]- and only 0.25 kcal mol^{-1} relative to the [o]-conformation occurs at a torsional angle close to 60°. At the B3LYP/cc-pVTZ level, however, the calculated torsional potential is exceedingly shallow around the [o]-conformation, certainly insufficiently deep to sustain a vibrational bound-state. The B3LYP/cc-pVTZ-calculated harmonic torsional frequency at the [o]-conformation of only 7 cm^{-1} is a further indication of this finding. For the two intermediate cases, MP (Figure 4a) and $TFMP^+$ (Figure 4d), torsional barriers of about 4.4 and 3.7 kcal mol^{-1} are predicted at the MP2 level and about 4.6 and 4.3 kcal mol^{-1} with B3LYP. A comparison of the torsional barriers based on MP2/cc-pVTZ calculations is given in Figure 4e. Already from

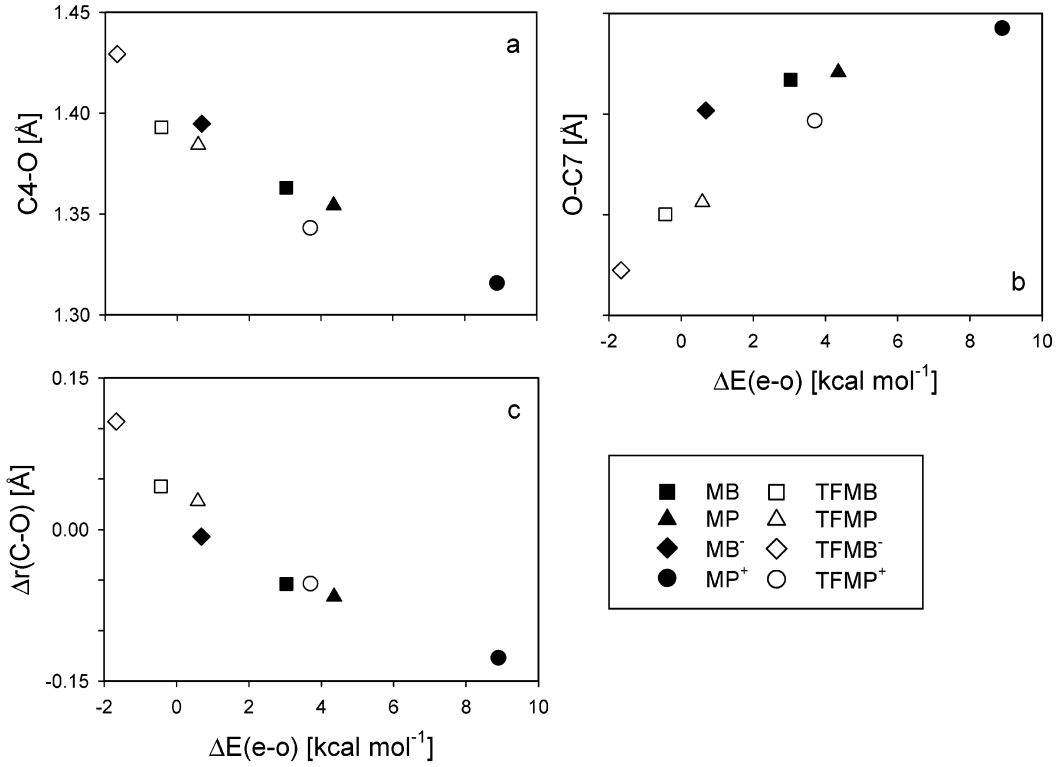

Figure 5. Plots of MP2/cc-pVTZ-optimized (a) C4−O, (b) O−C7, and (c) Δ*r*(C−O) versus Δ*E*(e−o).

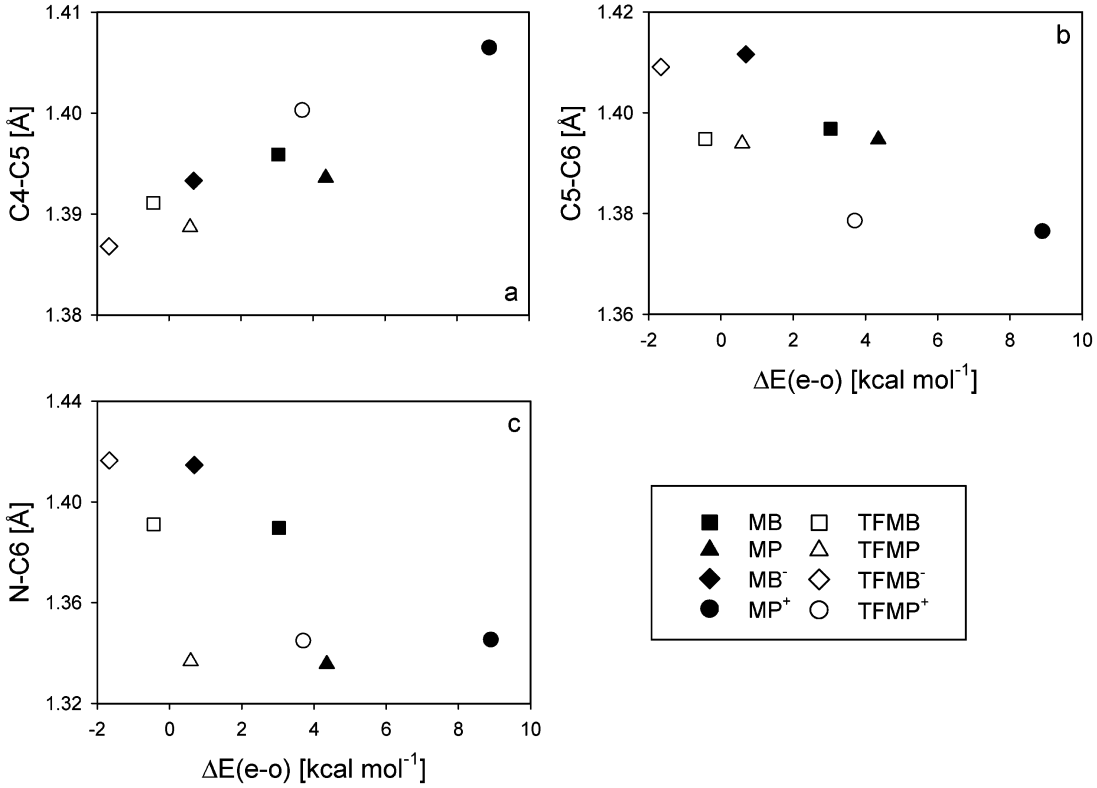

Figure 6. Plots of MP2/cc-pVTZ-optimized (a) C4−C5, (b) C5−C6, and (c) N−C6 versus Δ*E*(e−o).

visual inspection of Figure 4 it is evident that throughout the entire series MP2- and B3LYP-calculated torsional potentials are qualitatively very similar. Only at the saddle points at the [o]-conformation (a minimum in case of TFMP) are the B3LYP values slightly and systematically higher in energy than the corresponding MP2 values. The difference amounts to about 0.2−0.3 kcal mol^{-1} for MP, MP$^+$, and TFMP, and to 0.6 kcal mol^{-1} for TFMP$^+$.

The basis set dependence of the calculated torsional potentials is illustrated in Table 3. There, the MP2- and B3LYP-calculated energies as obtained at 30, 60 and 90° are reported relative to the energy minimum at the [e]-conformation for the Dunning basis sets of increasing size. For all four molecules and with B3LYP as well as with MP2, reasonable convergence is achieved at the cc-pVTZ stage. The difference between cc-pVTZ and cc-pVQZ is entirely negligible. The series including diffuse

functions (aug-) must necessarily converge toward the same limit, but the convergence is considerably slower. Overall, the B3LYP numbers are distinctly less sensitive to basis set extension. In the case of MP2, cc-pVDZ and aug-cc-pVDZ torsional potentials are still far from the cc-pVTZ curve. The very same trends have been observed in our earlier work on the torsional potentials of MB, MB^-, TFMB, and $TFMB^-$.[10] The B3LYP/cc-pVTZ and MP2/cc-pVTZ energies for these four molecules are also included in Table 3. Because of the flatness of the torsional potential, this difference between MP2/(aug-)cc-pVDZ and MP2/cc-pVTZ is particularly critical for the case of TFMP. With the (aug-)cc-pVDZ basis sets [e]- and [o]-conformations of TFMP would have been predicted to be nearly equienergetic, whereas with the cc-pVTZ and cc-pVQZ basis sets the energy difference between [e]- and [o]-conformations ΔE(e−o) amounts to about 0.6 kcal mol^{-1}.

The calculated Fourier fit coefficients V_n are compiled in Table 4. The fits have been extended up to V_8 in order to test whether the higher terms make significant contributions. V_8 is indeed negligible in all cases. Even V_6 is small and close to negligible in the cases of MP^+ and MP. In most cases, the important features of the torsional potential are well-described by V_2 and V_4, in the case of MP^+ by V_2 alone. The energy difference ΔE(e−o) is approximately equal to $V_2 + V_6$. The V_2 coefficient dominates and decreases from about 9 kcal mol^{-1} for MP^+ to 0.72 (MP2) and 0.89 (B3LYP) for TFMP, while those for MP and $TFMP^+$ are about midway between these extrema. The V_4 parameters are not negligible, but distinctly smaller.

In Figure 5, the MP2/cc-pVTZ-optimized single-bond distances for C4−O and O−C7 and their difference Δr(C−O), as obtained at the [e]-conformations, are plotted versus ΔE(e−o) for MP^+, $TFMP^+$, MP, and TFMP, and also for MB, MB^-, TFMB, and $TFMB^-$. For all three structural parameters the regular behavior of the $-OCH_3$ and $-OCF_3$-substituted series is quite impressive. The B3LYP/cc-pVTZ-optimized structural parameters and the corresponding energies give rise to practically identical plots and are therefore omitted. For both substituents, ΔE(e−o) decreases in the order pyridinium cation, pyridine, benzene, and phenyl anion and this decrease is accompanied by an increase in C4−O, a decrease in O−C7, and hence a strong decrease in Δr(C−O). Thereby, a large range of formal C−O single bonds is covered, both for C4−O and for O−C7, extending from about 1.31 to 1.45 Å. This range exceeds even that of a compilation of experimentally observed C−O distances in different saturated and unsaturated ethers.[24] The calculated energy differences between eclipsed and orthogonal conformations ΔE(e−o), mostly identical to the barrier heights, vary from about +9 to −1.7 kcal mol^{-1}, a range of more than 10 kcal mol^{-1} in relative stabilities.

Parallel to the contraction of the C4−O distance from a long C−O single bond toward a short C−O single bond with increasing double-bond character, the C−C distances in the aromatic ring are also systematically modified. With decreasing C4−O bond length they show an increasing distortion toward a quinoidic structure (see Figure 6 and Tables 1 and 2). This trend is particularly visible for C5−C6 (C2−C3) and also for C4−C5 (C3−C4). Since the IUPAC numbering for the substituted pyridine and benzene rings is different, that of the pyridine ring is used in this plot. The conventional explanation for the preference of an eclipsed conformation of MB, as opposed to an orthogonal conformation in ethylbenzene, is the occurrence of a stabilizing overlap of the oxygen lone pairs with the π-orbitals of the benzene ring. Thus, the variation of the structural distortions in these two series may also be rationalized by this conventional explanation, namely, an increasing degree of conjugation of the oxygen lone pairs with the π-orbitals of the aromatic ring upon going from the practically nonconjugated case of $TFMB^-$ to the strongly conjugated case of MP^+, where the term *conjugation* is meant as deformation toward a *quinoidic distortion* of the arene. In the former case, the [o]-conformation is the global minimum and the torsional potential is reminiscent of that of ethylbenzene.[10] In the latter case, the [e]-conformation is much more stable and the formal C4−O single bond has substantial double-bond character.

4. Conclusion

Large scale MP2 and B3LYP calculations were performed on the structure and torsional potentials of MP, TFMP, MP^+, and $TFMP^+$. From the data obtained in this work and from a comparison with analogous data on MB, TFMB, MB^-, and $TFMB^-$, the following conclusions may be drawn: (i) The para-substituted pyridines MP and TFMP, as well as the corresponding pyridinium cations MP^+ and $TFMP^+$, prefer the [e]-conformation. (ii) For MP, MP^+, and $TFMP^+$ the [o]-conformation is undoubtedly a saddle point. In the case of TFMP, the nature of the [o]-conformation could not be fully clarified. With both MP2 and B3LYP a formal minimum is obtained for the [o]-conformation, with a barrier close to 60°. The MP2 minimum is sufficiently deep to sustain a vibrational level, the B3LYP minimum is not. Overall, the torsional potential of TFMP is predicted to be very flat, with a barrier of only about 0.85 kcal mol^{-1} relative to the global minimum. (iii) For all eight species, the optimized distances of the two C−O bonds forming the ether linkage correlate very well with the energy difference between eclipsed and orthogonal conformations ΔE(e−o). (iv) Practically all the structural distortions taking place between the two extremes $TFMB^-$ and MP^+ may be understood by an increasing degree of conjugation of the oxygen lone pairs with the π-orbitals of the aromatic ring, thereby introducing an increasing degree of deformation toward a quinoidic structure.

Acknowledgment. The calculations were performed on the Linux-cluster SCHRÖDINGER I at the University of Vienna. The authors are grateful for ample supply of computer time on this installation.

References and Notes

(1) Allen, G.; Fewster, S. In *Internal Rotation in Molecules*; Orville-Thomas, W. J., Ed.; Wiley: New York, 1974; Chapter 8.
(2) Hester, R. E.; Owen, N. L. *Spectrochim. Acta A* **1969**, *25*, 343.
(3) Seip, H. M.; Seip, R. *Acta Chem. Scand.* **1973**, *27*, 4024.
(4) Onda, M.; Toda, A.; Mori, S.; Yamaguchi, I. *J. Mol. Struct.* **1986**, *144*, 47.
(5) Vincent, M. A.; Hillier, I. A. *Chem. Phys.* **1990**, *140*, 35.
(6) Spellmeyer, D. C.; Grootenhuis, P. D. J.; Miller, M. D.; Kuyper, L. F.; Kollman, P. A. *J. Phys. Chem.* **1990**, *94*, 4483−4491.
(7) Tsuzuki, S.; Houjou, H.; Nagawa, Y.; Hiratani, K. *J. Phys. Chem. A* **2000**, *104*, 1332.
(8) Kapustin, E. G.; Bzhezovsky, V. M.; Yagupolskii, L. M. *J. Fluorine Chem.* **2002**, *113*, 227.
(9) Gellini, C.; Moroni, L.; Muniz-Mirand, M. *J. Phys. Chem. A* **2002**, *106*, 10999.
(10) Klocker, J.; Karpfen, A.; Wolschann, P. *Chem. Phys. Lett.* **2003**, *367*, 566.
(11) Federsel, D.; Herrmann, A.; Christen, D.; Sander, D.; Willner, H.; Oberhammer, D. *J. Mol. Struct.* **2001**, *567−568*, 127.
(12) Shishkov, I. F.; Geise, H. J.; Van Alsenoy, C.; Khristenko, L. V.; Vilkov, L. V.; Senyavian, V. M.; Van der Veken, B.; Herrebout, W.; Lokshin, B. V.; Garkusha, O. G. *J. Mol. Struct.* **2001**, *567−568*, 339.

(13) Frisch, M. J.; Trucks, G. W.; Schlegel, H. B.; Scuseria, G. E.; Robb, M. A.; Cheeseman, J. R.; Zakrzewski, V. G.; Montgomery, J. A., Jr.; Stratmann, R. E.; Burant, J. C.; Dapprich, S.; Millam, J. M.; Daniels, A. D.; Kudin, K. N.; Strain, M. C.; Farkas, O.; Tomasi, J.; Barone, V.; Cossi, M.; Cammi, R.; Mennucci, B.; Pomelli, C.; Adamo, C.; Clifford, S.; Ochterski, J.; Petersson, G. A.; Ayala, P. Y.; Cui, Q.; Morokuma, K.; Malick, D. K.; Rabuck, A. D.; Raghavachari, K.; Foresman, J. B.; Cioslowski, J.; Ortiz, J. V.; Stefanov, B. B.; Liu, G.; Liashenko, A.; Piskorz, P.; Komaromi, I.; Gomperts, R.; Martin, R. L.; Fox, D. J.; Keith, T.; Al-Laham, M. A.; Peng, C. Y.; Nanayakkara, A.; Gonzalez, C.; Challacombe, M.; Gill, P. M. W.; Johnson, B. G.; Chen, W.; Wong, M. W.; Andres, J. L.; Head-Gordon, M.; Replogle, E. S.; Pople, J. A. *Gaussian 98*, revision A.11; Gaussian, Inc.: Pittsburgh, PA, 1998.

(14) Dunning, T. H., Jr. *J. Chem. Phys.* **1989**, *90*, 1007.

(15) Kendall, R. E.; Dunning, T. H., Jr.; Harrison, R. J. *J. Chem. Phys.* **1992**, *96*, 6796.

(16) Woon, D. E.; Dunning, T. H., Jr. *J. Chem. Phys.* **1993**, *98*, 1358.

(17) Woon, D. E.; Dunning, T. H., Jr. *J. Chem. Phys.* **1994**, *100*, 2975.

(18) Woon, D. E.; Dunning, T. H., Jr. *J. Chem. Phys.* **1995**, *103*, 4572.

(19) Møller C.; Plesset, M. S. *Phys. Rev.* **1934**, *46*, 618.

(20) Becke, A. D. *Phys. Rev. A* **1988**, *38*, 3098.

(21) Becke, A. D. *J. Chem. Phys.* **1993**, *98*, 5648.

(22) Lee, C.; Yang, W.; Parr, R. G. *Phys. Rev. B* **1988**, *37*, 785.

(23) Mielich, B.; Savin, A.; Stoll, H.; Preuss, H. *Chem. Phys. Lett.* **1989**, *167*, 200.

(24) Naumov, A. C. In *Stereochemical Applications of Gas-Phase Electron Diffraction*; Hargittai, I., Hargittai, M. Eds.; VCH Publishers: New York, 1988; Part B, p 93.